Effects of Angle of Attack on a Swept-Back Wing

S. C. Yen [a] and **C. M. Hsu** [b]
[a]National Taiwan Ocean University
Keelung, Taiwan 202, Republic of China
[b]National Taiwan University of Science and Technology
Taipei, Taiwan 106, Republic of China

Abstract

A NACA 0012 finite wing airfoil with a sweep-back angle of 15° and aspect ratio of 5 was utilized to study the effects of angle of attack (α) on the vortex shedding and aerodynamic coefficients. Frequency variations of unsteady structures in the wake were measured using a hot-wire anemometer. The frequency, projected Strouhal number (St_d), and projected Roshko number at various angles of attack were determined and discussed. The relationship between St_d and α can be equated as: $St_d = -9.7 \times 10^{-7} \alpha^3 + 1.6 \times 10^{-4} \alpha^2 - 9.6 \times 10^{-3} \alpha + 0.3$ for projected Reynolds number ranging from 2.0×10^4 to 3.3×10^4. Four characteristic surface flow patterns: separation bubble, leading-edge bubble, bubble burst, and turbulent separation were classified with α. Moreover, the behaviors of flow structures profoundly influenced the lift, drag, and moment coefficients. The lift coefficient (C_L) increases with α in the separation bubble and leading-edge bubble regimes. The maximum increase rate of lift coefficient $d(C_L)/d\alpha$ = 2.4/deg. appears in the leading-edge bubble regime and the maximum increase rate of drag coefficient $d(C_D)/d\alpha$ = 0.08/deg. appears in the bubble burst regime. The steep-descend of C_M at stalling in a straight-wing was eliminated by utilizing the swept-back wing.

Keyword: Swept-back wing, Vortex shedding, Aerodynamic performances

1. Introduction

Many physical phenomena, such as separation, reattachment, separation bubble, vortex, etc., emerge from the evolution of boundary layer on the wing suction surface. Therefore, the aerodynamic performance is closely related to the flow behaviors on wing surfaces. Furthermore, as shown in Fig. 1, the vortex shedding in the wake is swayed with the unstable wave generated from the separation of boundary layer. The bubble generally extends a large portion of the chord length and significantly changes the pressure distribution. The aerodynamic performance thus is significantly changed. Mueller *et al*. [1,2] experimentally studied the hysteresis loop in aerodynamic performance with the Lissaman 7769, Miley M06-13-128, and NACA 63_3-018 airfoils at low Reynolds numbers. Liu *et al*.[3] studied the of 30° swept-back wing and found that the lift increase results from the effect of the streak vortex not only on the inner panel but also on the outer panel. Also, the additional strake to the wing at low speed results in a nonlinear pitching moment variation at low and high angles of attack. The lift increment is decreased with an increase in Mach number at transonic speeds. The increase in the lift-drag ratio is due to the lift increase at low speeds and the drag decrease at supersonic speeds. Huang *et al*. [4] studied the NACA 0012 airfoil aerodynamic performance resulting from the change of the surface flow mode at different Reynolds numbers. The variations of surface flow due to the influence of the Reynolds number and free stream turbulence would inevitably lead to the modification of aerodynamic performance. It was found that the curve of the lift coefficient has the largest slope in the laminar separation regime, and the increased rate of the lift coefficient decreases when the separation bubble is formed. The stall happens in the turbulent separation regime. The drag coefficient, slightly decreasing in the laminar separation regime, remains almost a constant in the separation bubble regime, and increases in the transition regime.

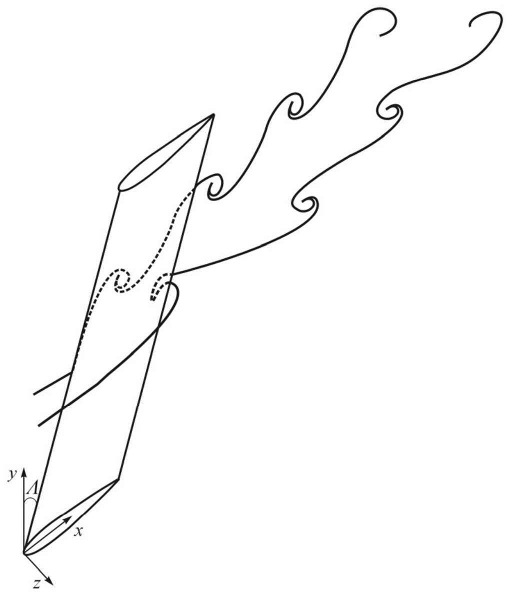

FIG 1. Schematic diagram of typical flow behavior on swept-back wing.

The stable vortex shedding in the wake of a swept-back wing is eventually initialized by the complex vortex on the wing surface. The unsteady flow behind the airfoil has profound influences on the airfoil performances. Roshko [5] found that the ordinary Strouhal number remained near constant, 0.21, 0.18, and 0.14 for a circular cylinder, 90° wedge, and flat plate, respectively, at Reynolds numbers between 10^3 and 10^5. These results indicated that the sharper the blockage body was, the lower the ordinary Strouhal number obtained. Zaman *et al*. [6] observed the low frequency oscillation of flow over an airfoil. They found that during deep stall, $\alpha \geq 18^o$, the usual bluff body shedding occurs at a Strouhal number of $St \approx 0.2$. But at the onset of static stall, at around $\alpha = 15^o$, a low frequency periodic oscillation was observed, with the corresponding St being an order of magnitude lower. Huang and Lin [7] probed the vortex shedding and shear-layer instability of the NACA 0012 wing. They revealed that the evolution of the vortex shedding behind the airfoil at low angle of attack is closely related to the behavior of the shear layer instabilities. At a high angle of attack, the low frequency shedding is superimposed by the high frequency shear layer instability waves. The characteristic modes, laminar, subcritical, transition, and supercritical modes of vortex shedding, are found in the chord Reynolds number/angle of attack domain.

A systematic survey of the surface flow patterns on a NACA 0012 swept-back wing in the range of Reynolds number from 30,000 to 130,000 has recently been reported by Yen and Hsu [8]. The characteristic domain of Yen *et. al*. is shown in Fig. 2 for reference. The boundary layer field is visualized with surface oil-flow techniques. Six characteristic flow regimes: *laminar separation*, *separation bubble*, *leading-edge bubble*, *bubble burst*, *turbulent separation* and *bluff-body wake*, are categorized and studied with considering the Reynolds numbers and angles of attack. These characteristic surface flow modes are closely related to the complex behavior of vortex shedding in the wake [8]. However, the properties of these characteristic flow modes and their influence on the aerodynamic performance were still not reported yet. In this study, the experimental results display the characteristic behaviors of surface flow modes and their influences on the aerodynamic performances and unsteady flow structures in the wakes of swept-back wings. The objectives of this research are: (1) to measure the aerodynamic coefficients using the six component balance, (2) to study the variation of moment coefficients between unswept and swept-back wings, and (3) to calibrate the shedding frequency of vortices in the wake using hot-wire anemometer measurements.

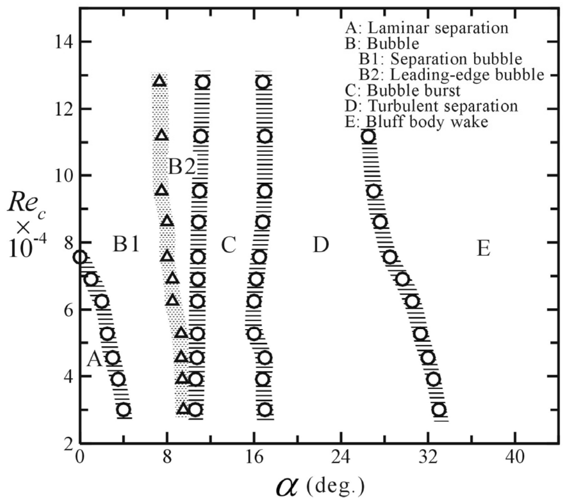

FIG 2. Characteristic flow regimes utilized in this study and Yen *et*. *al*. [8].

2. Experimental setup

As shown in Fig. 3, a closed-return wind tunnel was used to conduct the experiments. The wind tunnel had a test section of 60 cm × 60 cm × 120 cm. A polished aluminum alloy plate was utilized to be the floor and three highly transparent acrylic panels was applied to be the ceiling and side walls for photography and visualization. The operating velocity ranged from 0.56 to 60.0 m/s. In this velocity range, the maximum turbulence intensity was less than 0.2% and the non-uniformity of the average velocity profile across the cross-section was lower than 0.5%. During the experiments, the velocity of the approaching flow was monitored with a Pitot-static tube. When the free stream speeds were set to 5.0 m/s and 30.0 m/s, the thicknesses of the boundary layer [9] were about 4.03 mm and 1.65 mm, respectively. An aluminum plate with sharp leading and trailing edges was placed 50 mm above the floor of the test section to control the boundary layer thickness.

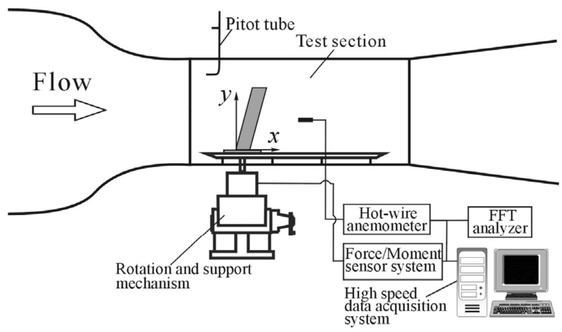

FIG 3. Experimental setup.

The airfoil model was made of stainless steel. The profile of the cross section was the NACA 0012, and the swept-back angle was 15 degrees. The chord length was 60 mm, and the span was 300 mm yielding the aspect ratio of 5. The airfoil model was mounted on a support and protruded through perpendicularly to the aluminum floor of the test section and the boundary layer thickness control plates.

The frequencies of the shed vortices in the wake region were detected by a TSI 1210-T1.5 constant-temperature hot-wire anemometer. The wire diameter and length were 5 μm and 1.5 mm, respectively, which ensured a dynamic response corresponding to the electronic square wave adjusted between 15 and 25 kHz. The hot-wire signals were fed simultaneously to an FFT analyzer and a high speed PC-based data acquisition system. The data acquisition system had a sample-and-hold function installed for multi-channel acquisition with no phase-lag. The sampling rate and the elapsed time of the data acquisition system were set to 16,000 samples/sec and 2 seconds, respectively, for the measurement of velocity properties.

The aerodynamic performances of the wing were taken via a JR^3 Universal Force-Moment System. The assembly of the wing model and balance was mounted on a rotary support. The rotary support had a resolution of 0.012 degree. The JR^3 balance had a monolithic six-degree-of-freedom force sensor. The output electronic signals of the sensor were sampled by a PC-based high-speed data acquisition system.

The measurement accuracy of the free stream velocity was affected primarily by the alignment of the Pitot tube and calibration of the pressure transducer. With the help of a synchronized micro pressure calibration system and careful alignment of the Pitot tube, the uncertainty of the free stream velocity was estimated to be 3%. The accuracy of the angle of attack was controlled to within 0.5%. The accuracy of the force-moment measurement was determined by the method used for mounting and calibration. The accuracy of the shedding frequency response depended on the recording period of the hot-wire system and the sampling rate of the FFT analyzer. The accuracy of the frequency was estimated to be within $\pm 0.75\%$ of the reading in this experiment. With the calibration matrix, the accuracies of lift and drag measurements were estimated to be about $\pm 1.5\%$ and $\pm 2.0\%$ of the reading.

3. Results and Discussion

Vortex shedding. The vortex shedding behaviors are measured by a hot-wire probe. The output signals of hot-wire anemometer are monitored by using an FFT analyzer in the time and frequency domains. To eliminate the effects of the wall and tip, this probe was located at $y/C = 2.5$, which is at the middle of the span, where y is the distance in the spanwise direction. Also, the collected signals in the x direction (streamwise) shows almost the same frequency profiles. Therefore, this probe was installed at $1 < x/C < 5$ to yield clear signals in the streamwise direction. These dimensions are measured from the wing root's leading edge. The frequencies of the unsteady motion in the wake of the swept wing that vary with free velocity are normalized and represented by nondimensional groups: projected Strouhal number $St_d = fd/u_\infty$, and Roshko number of vortex shedding $Ro_d = fd^2/v$, where v is the kinetic viscosity of air. Figure 4 plots variations of the frequency, and projection Strouhal number and the projection Roshko number of vortex shedding from the swept-back wing. Fig 4(a) shows the angle of attack increase, the frequency decrease. In Fig. 4(b), the projection Strouhal number rises abruptly with the angle of attack in vary projection Reynolds numbers. At $\alpha = 0$ deg., the maximum value of the projection Strouhal number is 0.42. In the high angle of attack, the projection Strouhal number (St_d) and angle of attack can be related as: $St_d = -9.7 \times 10^{-7}\alpha^3 + 1.6 \times 10^{-4}\alpha^2 - 9.6 \times 10^{-3}\alpha + 0.3$ for projected Reynolds number 2.0×10^4 to 3.3×10^4. In the constant projection Reynolds number, the projection Roshko number is proportional to the angle of attack as shown in Fig. 4(c).

Aerodynamic performances. The aerodynamic performance results are shown in Figures 4 by plotting the lift coefficient C_L, drag coefficient C_D, and moment coefficient C_M as the functions of angle of attack being subject to the chord Reynolds number of 1.0×10^5. Figure 5(a) shows that the lift coefficient C_L increases monotonically with the increase of angle of attack when the surface flow on the suction surface is in the regimes of separation bubble, and leading-edge bubble. The lift coefficient increases

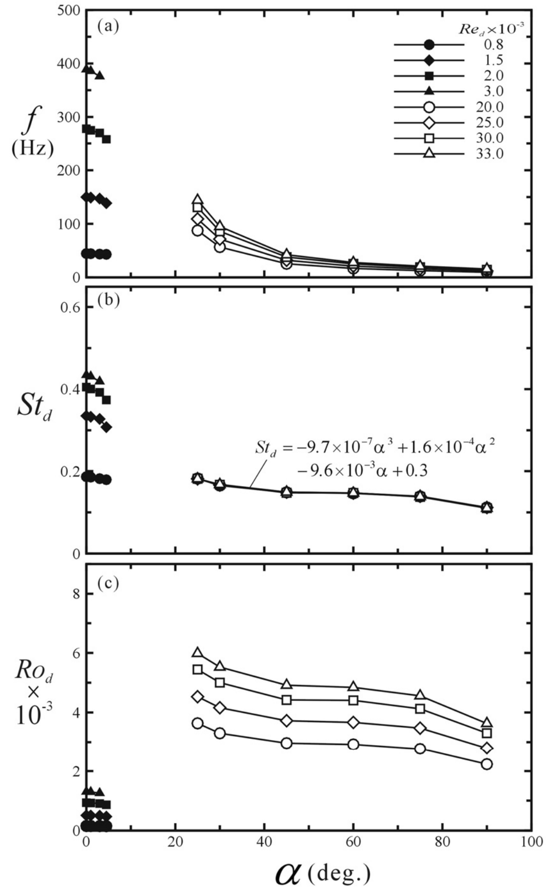

FIG 4. Variations of angle of attack with (a) frequency, (b) projected Strouhal number St_d, and (c) projected Roshko number Ro_d.

with angle of attack in the separation bubble and leading-edge bubble regimes and the maximum increase rate of lift coefficient $d(C_L)/d\alpha = 2.4$/deg. appears in the leading-edge bubble regime. The maximum value of C_L is about 1.22 at the leading-edge bubble regime. The lift begins to decrease when the surface flow is in the bubble burst regime. In the bubble burst regime, the reattached turbulent surface flow separates again to form the second separation. The second separation line moves toward the leading edge with the increase of angle of attack. With the forward motion of the second separation line, the wing goes into a stall. The minimum C_L value is about 0.88. The lift increases again as the angle of attack is further increased to the turbulent separation regime. This lift increase phenomenon is induced from the reaction of the scavenging effect on the suction surface and impact pressure on the pressure surface.

Figure 5(b) shows the C_D, the value of the drag coefficient, in the separation bubble regime. Although the bubble moves toward the leading edge and reduces its size with the increase of the angle of attack. The reduction of the shear stress decreases the shear drag and compensates for the increase of the form drag. The drag coefficient hence does not vary much in the separation bubble regime. In the leading-edge bubble regime, the increase of skin-friction and decrease of bubble size in this regime lead to a jump in the drag coefficient. In the bubble burst regime, the reattached turbulent surface flow creates a large skin friction on the suction surface. The maximum increase rate of drag coefficient $d(C_D)/d\alpha$ = 0.08/deg. appears in the bubble burst regime. The drag coefficient increases almost linearly with the increase of the angle of attack in the regime of turbulent separation, resulting from the significant increase of the form drag.

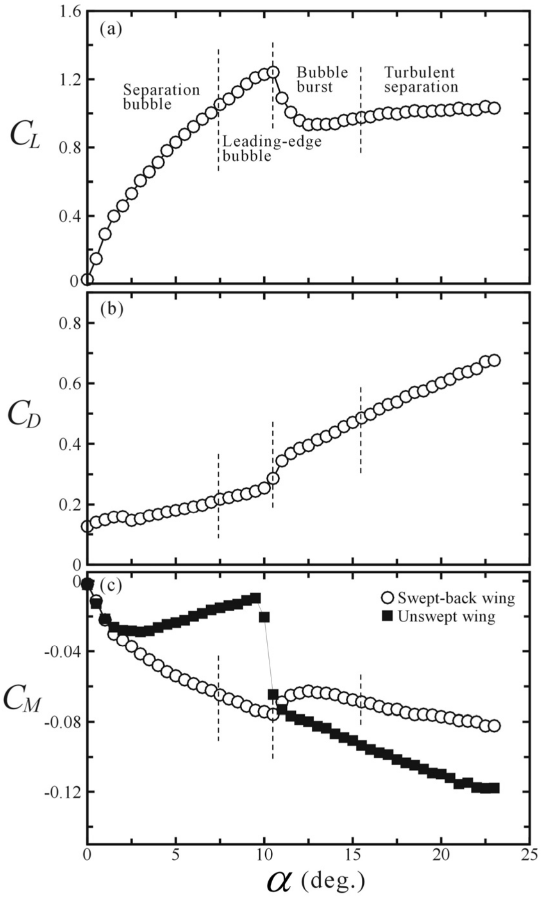

FIG 5. Aerodynamic performances of swept-back wing: (a) lift coefficient, (b) drag coefficient, and (c) moment coefficient, respectively. $Re_c = 1.0 \times 10^5$ for all cases.

Figure 5(c) shows the distribution of C_M, the quarter-chord moment coefficient, as a function of α at $Re_c = 10^5$. In the separation regime, C_M decreases as α increases. In the leading-edge bubble regime, C_M increases as α increases due to the sudden loss of lift (i.e. stalling). In the regime of bubble burst, C_M reaches its local maximum resulting from the increase of form drag. In the turbulent separation regime, C_M decreases as α increases due to the large increase of form drag. Furthermore, Fig. 5(c) displays that the steep-descend of C_M at stalling in straight-wing was eliminated with utilizing the swept-back wing. Figure 6 shows the resultant position of the lift and drag. The moving of the resultant position explain the change of C_M curve shown in Fig. 5(c).

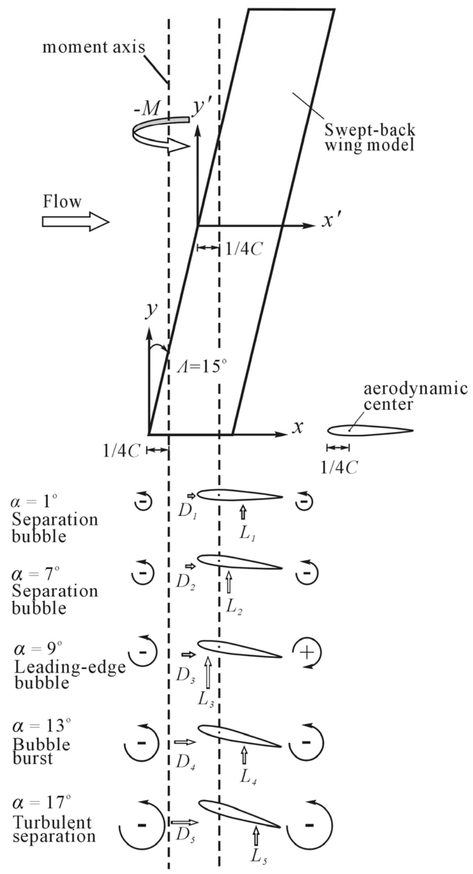

FIG 6. Schematic of the aerodynamic effect on pitch-moment.

4. Concluding Remarks

The characteristics of the aerodynamic performances, and the vortex shedding of a finite swept-back airfoil are experimentally studied in this paper. The following conclusions are drawn from the results and discussion.

1) The frequency, projected Strouhal number, and projected Roshko number at various angles of attack were determined and discussed. Projected Strouhal number (St_d) and angle of attack can be related as: $St_d = -9.7 \times 10^{-7} \alpha^3 + 1.6 \times 10^{-4} \alpha^2 - 9.6 \times 10^{-3} \alpha + 0.3$ for projected Reynolds number 3×10^3 to 3.3×10^4.

2) The lift coefficient (C_L) increases with angle of attack in the separation bubble and leading-edge bubble regimes and the maximum increase rate of lift coefficient $d(C_L)/d\alpha$ = 2.4/deg. appears in the leading-edge bubble regime. The maximum increase rate of drag coefficient $d(C_D)/d\alpha$ = 0.08/deg. appears in the bubble burst regime.

3) The steep-descend of C_M at stalling in straight-wing was eliminated with utilizing the swept-back wing.

5. Nomenclature

b	span of airfoil, 30 cm
C	chord length of wing, 6 cm
C_L	lift coefficient (= L/qbC)
C_D	drag coefficient (= D/qbC)
C_M	moment coefficient of pitching about quarter chord (= M/qbC)
D	drag force, measured by balance in free stream direction
L	lift force, measured by balance in cross free stream direction
M	pitching moment about quarter chord location
q	dynamic pressure of free stream (= $\rho u^2/2$)
d	length of wing-section projection on cross-stream plane
f	frequency of instabilities in wake region (Hz)
Re_d	Reynolds number based on cross-stream projection of wing section (= ud/ν)
Ro_d	Roshko number based on cross-stream projection of vortex shedding (= $f\,d^2/\nu$)
St_d	Strouhal number based on cross-stream projection of vortex shedding (= $f\,d/u$)
α	angle of attack
Λ	swept-back angle
ρ	density of air stream
ν	kinetic viscosity of air stream

6. Reference

[1] Mueller, T. J., Pohlen, L. J., Conigliaro P. E., and Jansen, B. J., "The influence of free-stream dimensional on low Reynolds number airfoil experiments," *Experiments in Fluids*, Vol. 1, 1983, pp. 3-14.

[2] Mueller, T. J., "The influence of laminar separation and transition on the low Reynolds number airfoil hysteresis," *Journal of Aircraft*, Vol. 22, No. 9, 1985, pp. 763-770.

[3] Liu, M. J., Lü, Z. Y., Qiu, C. H., Su, W. H., Gao, X. K., Deng, X. Y., and Xiong, S. W., "Flow Patterns and Aerodynamics Characteristic of a Wing-Strake Configuration," *Journal of Aircraft*, Vol. 17, No. 5, 1980, pp. 332-338.

[4] Huang, R. F., Shy, W. W., Lin, S. W., and Hsiao, F.-B., "Influence of Surface Flow on Aerodynamic Loads of a Cantilever Wing," *AIAA Journal*, Vol. 34, No. 3, 1996, pp. 527-532.

[5] Roshko, A., "On the Wake and Drag of Bluff Bodies," *Journal of the Aerospace Science*, Vol. 22, 1955, pp. 124-135.

[6] Zaman, K. B. M. Q., McKinzie, D. J., and Rumsey, C. L., "A Natural Low-Frequency Oscillation of the Flow over an Airfoil near Stalling Conditions," *Journal of Fluid Mechanics*, Vol. 202, 1989, pp. 403-442.

[7] Huang, R. F. and Lin, C. L., "Vortex Shedding and Shear-Layer Instability of Wing at Low-Reynolds Numbers," *AIAA Journal,* Vol. 33, No. 8, 1995, pp. 1398-1430.

[8] Yen, S. C. and Hsu, C. M., "Influence of Boundary Layer Behavior on Aerodynamic Coefficients of a Swept-Back Wing," *ASME Journal of Fluids Engineering*, Vol. 129, No. 6, 2007, pp. 674-681.

[9] Shames, I. H., *Mechanics of fluid*, 3rd ed., McGraw-Hill, Inc., Singapore, 1992, pp. 632.

[10] Hoerner, S. F. and Borst, H. V., *Fluid Dynamic Lift*, Mrs. Liselotte A. Hoerner, Brick Town, New Jersey, 1975, pp.422-423 and 156-158.